Transactions of the Materials Research Society of Japan 31[2] 279-282 (2006)

Synthesis and Structural Characterization of $LiNi_{1/2-x}Mg_xMn_{1/2}O_2$ and $LiNi_{1/3-x}Mg_xCo_{1/3}Mn_{1/3}O_2$

Yasuhiro Fujii [a,b], Hiroshi Miura [a], Naoto Suzuki [a], Takayuki Shoji [a], and Noriaki Nakayama [b]
[a] Tosoh Co., Ltd, 4560 Kaisei-cho, Syunan, Yamaguchi 746-8501, Japan
Fax: 81-834-63-9896, e-mail: ya_fujii@tosoh.co.jp
[b] Faculty of Engineering, Yamaguchi University, 2-16-1 Tokiwadai, Ube, 755-8611, Japan
Fax: 81-836-85-9601, e-mail: nakayamn@yamaguchi-u.ac.jp

$LiNi_{1/2-x}Mg_xMn_{1/2}O_2$ ($0.0 \leqq x \leqq 0.1$) and $LiNi_{1/3-x}Mg_xCo_{1/3}Mn_{1/3}O_2$ ($0.0 \leqq x \leqq 1/3$) solid solutions have been synthesized and their crystal structures have been investigated. Both systems adopt α-$NaFeO_2$-type layered rock-salt structure. Powder x-ray diffraction (XRD) patterns of $LiNi_{1/2-x}Mg_xMn_{1/2}O_2$ show fairly sharp (1/3,1/3, L) superlattice reflections (L=0,1,2,3) indicating an in-plane [$\sqrt{3}\times\sqrt{3}$] R30°-type ordering and the almost regular layer stacking with some staking faults. The XRD patterns of $LiNi_{1/3-x}Mg_xCo_{1/3}Mn_{1/3}O_2$ do not show the sharp superlattice peaks, but show diffuse scatterings with a intensity maximum at around 2θ = 21° corresponding to the (1/3,1/3,0) superlattice reflection of an in-plane [$\sqrt{3}\times\sqrt{3}$] R30°-type ordering. Electron diffraction patterns also indicate that the [$\sqrt{3}\times\sqrt{3}$] R30°-type ordered layers are stacked almost randomly in $LiNi_{1/3-x}Mg_xCo_{1/3}Mn_{1/3}O_2$.

Key words: Li-ion batteries, superlattice, layer stacking

1. Introduction

Recently, compounds in the Li-Ni-Mn-O and Li-Ni-Co-Mn-O systems have been proposed as possible alternatives to $LiCoO_2$ widely used in current Li-ion batteries [1-3]. $LiNi_{1/2}Mn_{1/2}O_2$ and $LiNi_{1/3}Co_{1/3}Mn_{1/3}O_2$ are the most possible candidates [4,5]. The remarkable properties of these materials are related to the valence state of transition metals; 2+, 3+, and 4+ for Ni, Co, and Mn, respectively [6,7]. Both compounds have been confirmed to adopt layered rock-salt type structures based on α-$NaFeO_2$ type one with a space group symmetry of $R\bar{3}m$. Some superstructure models for the cationic ordering in the α-$NaFeO_2$ type structure have been reported [8-10]. For $LiNi_{1/2}Mn_{1/2}O_2$, G. Ceder et al. have proposed a [$2\sqrt{3}\times 2\sqrt{3}$]-type ordering in the transition metal layers based on the Li-NMR measurements [8]. On the other hand, T. Ohzuku et al. have proposed a [$\sqrt{3}\times\sqrt{3}$] R30°-type cationic ordering for $LiNi_{1/3}Co_{1/3}Mn_{1/3}O_2$ with a space group symmetry of $P3_112$ [9,10]. No strong evidence has been reported for both superstructures and the cationic arrangements in these phases are still controversial. One of the reasons why the structures and the cationic distribution have not confirmed adequately is the similarity of x-ray atomic scattering factors among Ni, Co, and Mn.

The Mg-substitution for Ni in $LiNi_{1/2}Mn_{1/2}O_2$ and $LiNi_{1/3}Co_{1/3}Mn_{1/3}O_2$ is interesting in the above context. The x-ray atomic scattering factor of Mg is much smaller than that of transition metals. If $LiMg_{1/2}Mn_{1/2}O_2$ and $LiMg_{1/3}Co_{1/3}Mn_{1/3}O_2$ can be synthesized, their cationic orderings may be easily characterized by normal powder XRD and they must show some resemblances to those in $LiNi_{1/2}Mn_{1/2}O_2$ and $LiNi_{1/3}Co_{1/3}Mn_{1/3}O_2$. In fact, $Li_2NiMn_3O_8$ and $Li_2MgMn_3O_8$ with the spinel structures show the same cationic ordering in the B-sublattice. Then we have tried to prepare the solid solutions in the pseudo-binary $LiNi_{1/2-x}Mg_xMn_{1/2}O_2$ and $LiNi_{1/3-x}Mg_xCo_{1/3}Mn_{1/3}O_2$ systems prepared in order to increase the difference in atomic scattering factors among cations and characterized them by using powder a XRD and an electron diffraction (ED).

2.Experimental

Samples with nominal composition of $LiNi_{1/2-x}Mg_xMn_{1/2}O_2$ (x=0.0, 0.05, 0.1, 0.2, and 0.3) and $LiNi_{1/3-x}Mg_xCo_{1/3}Mn_{1/3}O_2$ (x=0.0, 0.05, 0.1, 0.2, and 1/3) samples were prepared by heating the mixtures of lithium hydroxide and mixed metal hydroxide. Calcinations were made for 12h in air stream at 1000℃ for $LiNi_{1/2-x}Mg_xMn_{1/2}O_2$ and at 900 ℃ for $LiNi_{1/3-x}Mg_xCo_{1/3}Mn_{1/3}O_2$. Excess lithium hydroxide was added in an attempt to compensate for Li loss by volatilization. The heating and cooling rate of 100℃ h^{-1} was applied for all temperature settings. Samples were identified and characterized by powder XRD and ED. For ED measurements, samples were dispersed in ethanol by applying the ultrasonic wave and were collected on a holly micro grid supported on a copper grid mesh. A field emission type TEM (JEOL JEM2010F) operated at 200kV was used. The chemical composition, and the average oxidation state of transition metals were determined by ICP-AES, and iodometric titration, respectively [11]. The chemical compositions of all samples measured by ICP-AES were almost identical to the expected.

3. Results and discussion

3.1 $LiNi_{1/2-x}Mg_xMn_{1/2}O_2$

Powder XRD patterns of $LiNi_{1/2-x}Mg_xMn_{1/2}O_2$ are shown in Fig. 1. They are characteristic of a layered rock-salt type structure. However, several peaks of impurity phase tend to appear for x = 0.2 and 0.3, as marked by arrows. Therefore, Mg atoms are soluble up to x=0.1 in the $LiNi_{1/2-x}Mg_xMn_{1/2}O_2$ system. At the present stage, the impurity phases are unknown. As shown in Fig. 2, parameters, a and c in the hexagonal setting increase monotonically as a function of Mg substitution. Fig. 3 shows enlarged XRD pattern for single phase samples with x=0, 0.05, and 0.10, of which ordinate shows logarithmic intensity. They show weak but fairly sharp superlattice peaks, which can be indexed as (1/3, 1/3, *L*) reflections with *L*= 0, 1, 2, and 3 based on the α-$NaFeO_2$-type $R\bar{3}m$ lattice in the hexagonal setting. These peaks indicate a $[\sqrt{3}\times\sqrt{3}]$ R30°-type cationic ordering similar to the one in Li_2MnO_3 (monoclinic *C2/m*, [12]). ED patterns also showed superlattice spots indicating a $[\sqrt{3}\times\sqrt{3}]$ R30°-type ordering.

Even in the case of the sample with x=0.0, the XRD pattern shows very weak superlattice peaks at the similar positions and the intensity of superlattice peaks increases with x increasing. Therefore the superstructure is probably due to the ordering of divalent (Mg, Ni) and tetra-valent (Mn) atoms. The peak width and peak shape suggest some stacking disorder in the superlattice. The detailed structural characterizations by using Rietveld method and lattice image observations are in progress for the sample with x=0.10.

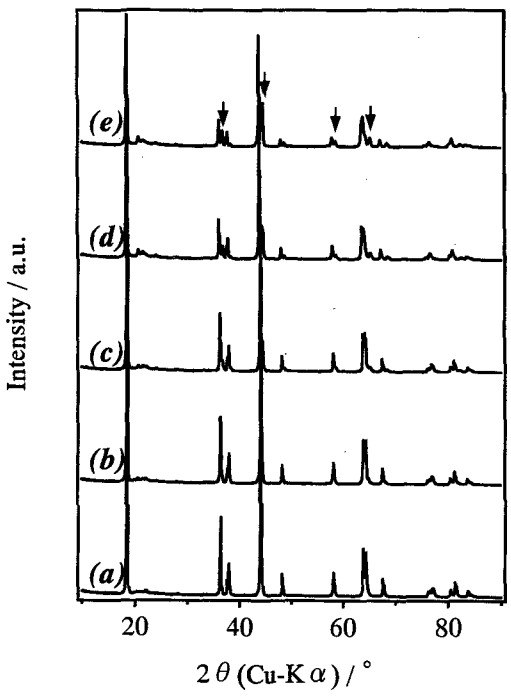

Figure 1. XRD patterns of $LiNi_{1/2-x}Mg_xMn_{1/2}O_2$ samples prepared at 1000℃ for 12h in air stream. (a) x=0.0, (b) x=0.05, (c) x=0.1, (d) x=0.2, and (e) x=0.3

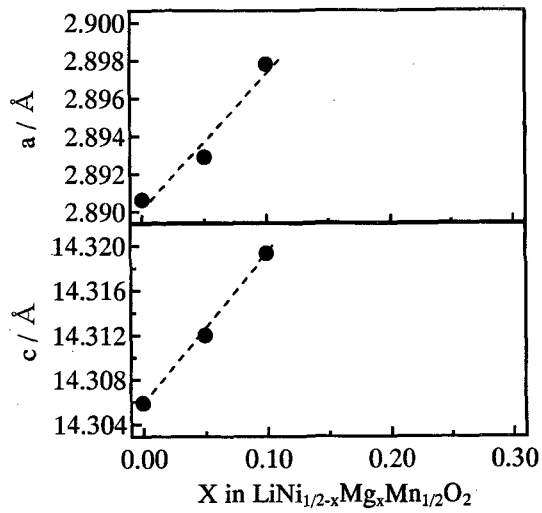

Figure 2. Lattice parameters of α-$NaFeO_2$ type phase for $LiNi_{1/2-x}Mg_xMn_{1/2}O_2$ prepared at 1000℃ for 12h in air stream.

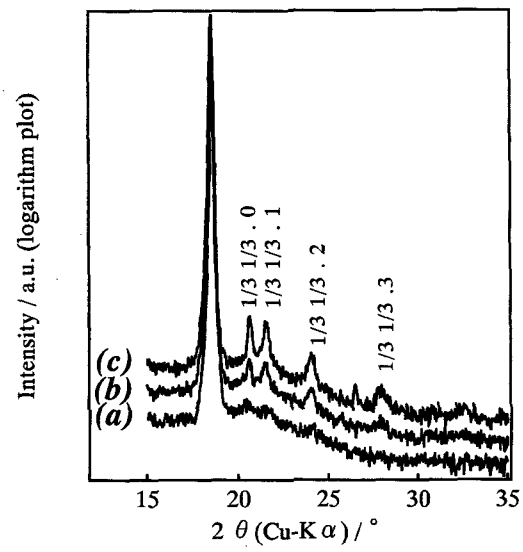

Figure 3. Enlarged XRD patterns of single phase $LiNi_{1/2-x}Mg_xMn_{1/2}O_2$ with (a) x=0.0, (b) x=0.05, and (c) x=0.1. The ordinate shows the logarithmic intensity.

3.2 $LiNi_{1/3-x}Mg_xCo_{1/3}Mn_{1/3}O_2$

XRD patterns in Fig. 4 indicate that all of the samples in the $LiNi_{1/3}Co_{1/3}Mn_{1/3}O_2$ - $LiMg_{1/3}Co_{1/3}Mn_{1/3}O_2$ solid solution system adopt α-$NaFeO_2$ type structure. No peaks of impurity phases were detected. The lattice parameters in the hexagonal setting are plotted in Fig. 5 as a function of the Mg composition x. With increasing Mg composition, the a-axis length decreases monotonically and oppositely the c-axis length increases. Fig. 6 shows the average valence of transition metals measured by an iodometric titration. Experimental valences agree with the calculated ones from the composition. The complete solid solutions are obtained in the $LiNi_{1/3-x}Mg_xCo_{1/3}Mn_{1/3}O_2$ system.

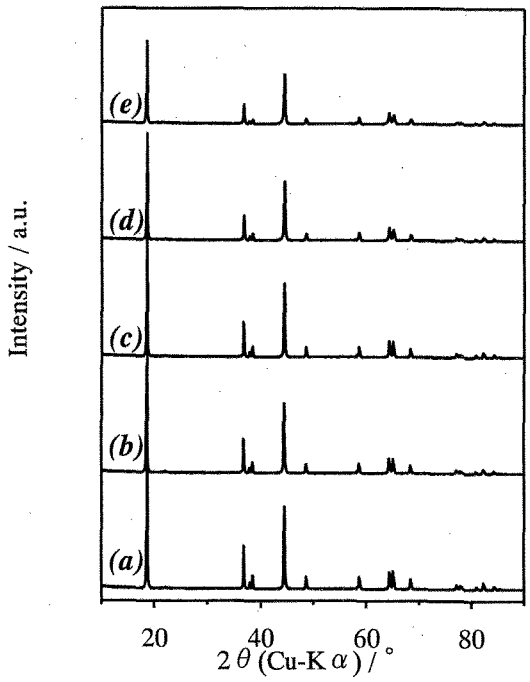

Figure 4. XRD patterns of $LiNi_{1/3-x}Mg_x$-$Co_{1/3}Mn_{1/3}O_2$ samples prepared at 900℃ for 12h in air stream.
(a) x=0.0, (b) x=0.05, (c) x=0.1, (d) x=0.2, and (e) x=1/3

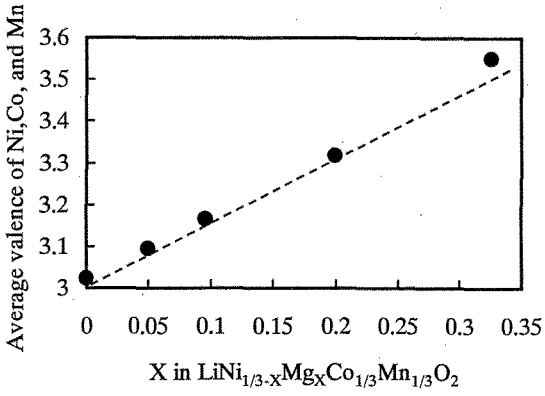

Figure 6. The average valence of transition metals for $LiNi_{1/3-x}Mg_xCo_{1/3}Mn_{1/3}O_2$ samples. The dotted line indicates the calculated value from the composition.

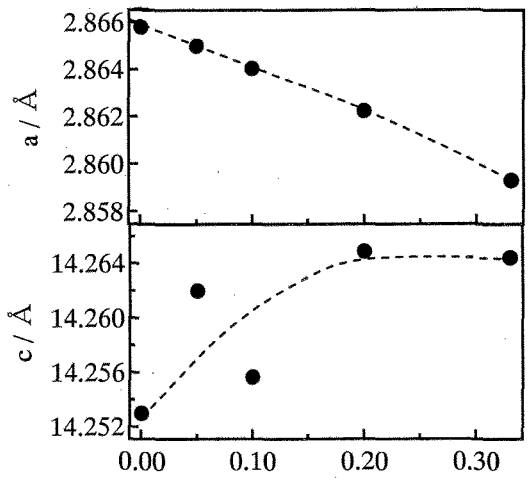

Figure 5. Lattice parameters of $LiNi_{1/3-x}Mg_x$-$Co_{1/3}Mn_{1/3}O_2$ prepared at 900℃ for 12h in air stream.

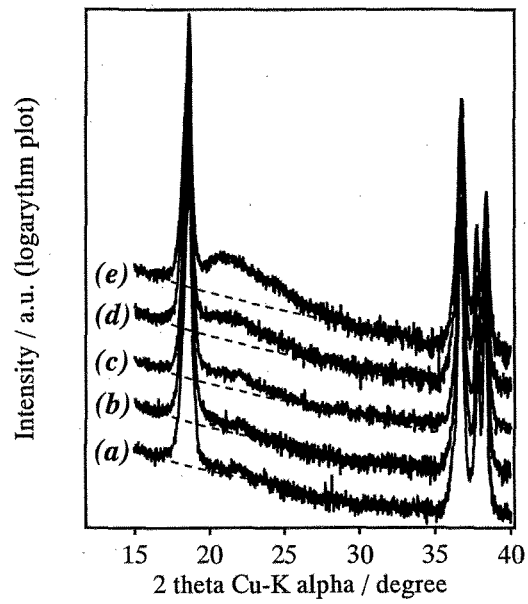

Figure 7. XRD patterns of $LiNi_{1/3-x}Mg_x$-$Co_{1/3}Mn_{1/3}O_2$ samples prepared at 900℃ for 12h in air stream.
(a) x=0.0, (b) x=0.05, (c) x=0.1, (d) x=0.2, and (e) x=1/3

However, no sharp superlattice reflections indicating $[\sqrt{3}\times\sqrt{3}]$ R30°-type ordering as expected from the $P3_112$ model structure proposed by Ohzuku et al. was observed. Figure 7 shows XRD patterns carefully measured using a sample folder made of quartz single crystal, to avoid the background intensity from sample holder. The XRD pattern of $LiMg_{1/3}Co_{1/3}Mn_{1/3}O_2$ shows fairly intense diffuse scattering in the 2θ range from 18 to 25°. The intensity of the diffuse scattering decreases with decreasing the Mg composition. TEM observations indicated that the diffuse scattering was not caused by the amorphous component but was originated from the two dimensional cationic ordering.

Figure 8 shows [00.1] and [11.0] zone ED patterns (EDPs) of two end-members, $LiMg_{1/3}Co_{1/3}Mn_{1/3}O_2$ and $LiNi_{1/3}Co_{1/3}Mn_{1/3}O_2$. The indexes are in the hexagonal setting. No amorphous component was observed during TEM observation. The [00.1] zone EDPs show the extra spots due to the $[\sqrt{3}\times\sqrt{3}]$R30°-type ordering in the transition metal layers. Extra spots in the EDP of $LiMg_{1/3}Co_{1/3}Mn_{1/3}O_2$ are more intense than those of $LiNi_{1/3}Co_{1/3}Mn_{1/3}O_2$. The smaller electron scattering factor of Mg compared with transition metals has enhanced the intensity of superlattice spots. The [11.0] zone EDPs show the diffuse streaks along the c* axis, indicating the severe stacking disorder of a $[\sqrt{3}\times\sqrt{3}]$ R30°-type ordered transition metal layers.

The positions of diffuse streaks in the reciprocal c*-plane agree with the extra spots in the observed [00.1] EDPs. The diffuse scattering in the powder XRD patterns agree with the two dimensional $[\sqrt{3}\times\sqrt{3}]$ R30°-type ordering observed by ED. The intensity maximum at around 21° give a d-value of 4.2Å, which agree with the lattice spacing d (1/3, 1/3, 0) = (3/2)a = 4.23Å. The diffuse and two dimensional nature of the diffraction patterns indicate that the $[\sqrt{3}\times\sqrt{3}]$ R30°-type ordered transition metal layers are stacked almost randomly. The formation of the complete solid-solution suggests a similar structure for $LiNi_{1/3}Co_{1/3}Mn_{1/3}O_2$, although there may exist some difference in the order parameters.

4. Conclusions

Solid solutions with layered α-$NaFeO_2$-type structure, $LiNi_{1/2-x}Mg_xMn_{1/2}O_2$ ($0.0 \leqq x \leqq 0.1$) and $LiNi_{1/3-x}Mg_xCo_{1/3}Mn_{1/3}O_2$ ($0.0 \leqq x \leqq 0.33$), have been successfully synthesized. In the former system, the Mg substitution enhances the intensity of the superlattice reflections due to the $[\sqrt{3}\times\sqrt{3}]$ R30°-type ordering. However the complete Mg-substitution of Ni was not attained. In the latter system, the completely Mg-substituted sample, $LiMg_{1/3}Co_{1/3}Mn_{1/3}O_2$, was obtained. Powder XRD pattern of $LiMg_{1/3}Co_{1/3}Mn_{1/3}O_2$ shows a broad and diffuse peak at around the superlattice reflections expected for the $[\sqrt{3}\times\sqrt{3}]$ R30°-type ordering. ED patterns also show the diffuse streaks along the reciprocal c*-axis. The positions of the diffuse streaks in the reciprocal c*-plane agree with the the $[\sqrt{3}\times\sqrt{3}]$ R30°-type ordering. The ordering in $LiMg_{1/3}Co_{1/3}Mn_{1/3}O_2$ is two dimensional probably because of the stacking disorder, similarly to the turbo-static structure of graphite [13]. The detailed structural characterizations by using powder XRD and high resolution TEM lattice image observations are in progress.

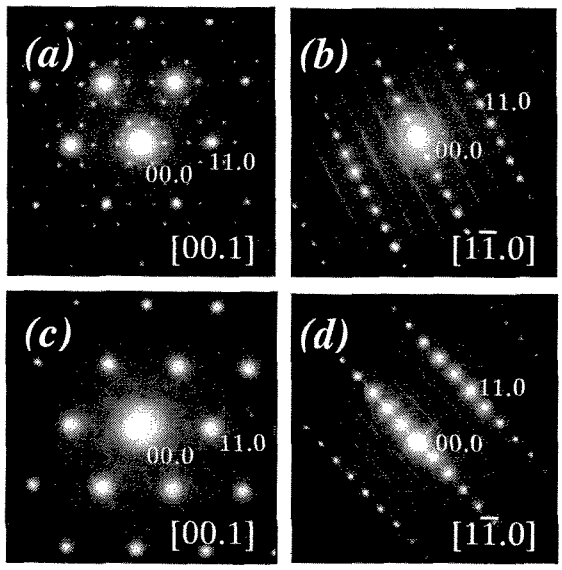

Figure 8. [00.1] zone and [1$\bar{1}$.0] zone ED patterns of $LiMg_{1/3}Co_{1/3}Mn_{1/3}O_2$ (a, b) and $LiNi_{1/3}Co_{1/3}Mn_{1/3}O_2$ (c, d). The diffraction spots have been indexed assuming the $R\bar{3}m$ structure in hexagonal setting.

References

[1] E. Rossen, C.D.W. Jones, and J.R. Dahn, *Solid State Ionics*, **57**, 311-318 (1992)
[2] Z. Lu, D. D. Macneil, and J. R. Dahn, *Electrochem. Solid-state Lett.*, **4**, 200 (2001)
[3] Y. Koyama, I. Tanaka, H. Adachi, Y. Makimura and T. Ohzuku, *J. Power Sources*, **119-121**, 644-648 (2003)
[4] T.Ohzuku and Y.Makimura, *Chem. Lett.*, 744-745 (2001).
[5] N. Yabuuchi, and T. Ohzuku, *J. Power Sources*, **119-121**, 171-174 (2003)
[6] H.Kobayashi, H. Sakaebe, H. Kageyama, K. Tatsumi, Y. Arachi, and T. Kageyama *J. Mater. Chem.*, **13**, 590-595 (2003)
[7] Y. Koyama, I. Tanaka, H. Adachi, Y. Makimura and T. Ohzuku, *J. Power Sources*, **119-121**, 644-648 (2003)
[8] A. Van der Ven, G.Ceder, *Electrochem. Commun.*, **6**, 1045 (2004)
[9] N. Yabuuchi, Y Koyama, N. Nakayama, and T. Ohzuku, J. Electrochem. Soc., 152, A1434 (2005)
[10] P.S. Whitfield, I.J. Davidson, L.M.D. Cranswick, I.P. Swainson, and P.W. Stephens, *Solid State Ionics*, **176**, 463 (2005)
[11] L. D. dyyer, B. S. Borie, Jr., and G. P. Smith, *J. American Chem. Soc.*, (1954)
[12] Von M. Jansen and R. Hoppe, *Z. Anorg. Allg. Chem.* **397**, 279-289 (1973)
[13] B. E. Warren, *Phys. Rev.* **59**, 693-698 (1941)

(Received January 15, 2006; Accepted March 30, 2006)